Title

SPINODAL ORDERING BEYOND THE LIFSHITZ POINT IN Cu3Pd OBSERVED BY HIGH-VOLTAGE ELECTRON MICROSCOPY

Authors

Takeda, S.
Kulik, J.
Fontaine, D. de

Publication Date

1986-08-01

LBL-22035
Preprint

Lawrence Berkeley Laboratory
UNIVERSITY OF CALIFORNIA

Materials & Molecular Research Division

Submitted to Acta Metallurgica

SPINODAL ORDERING BEYOND THE LIFSHITZ POINT
IN Cu_3Pd OBSERVED BY HIGH-VOLTAGE ELECTRON MICROSCOPY

S. Takeda, J. Kulik, D. de Fontaine

August 1986

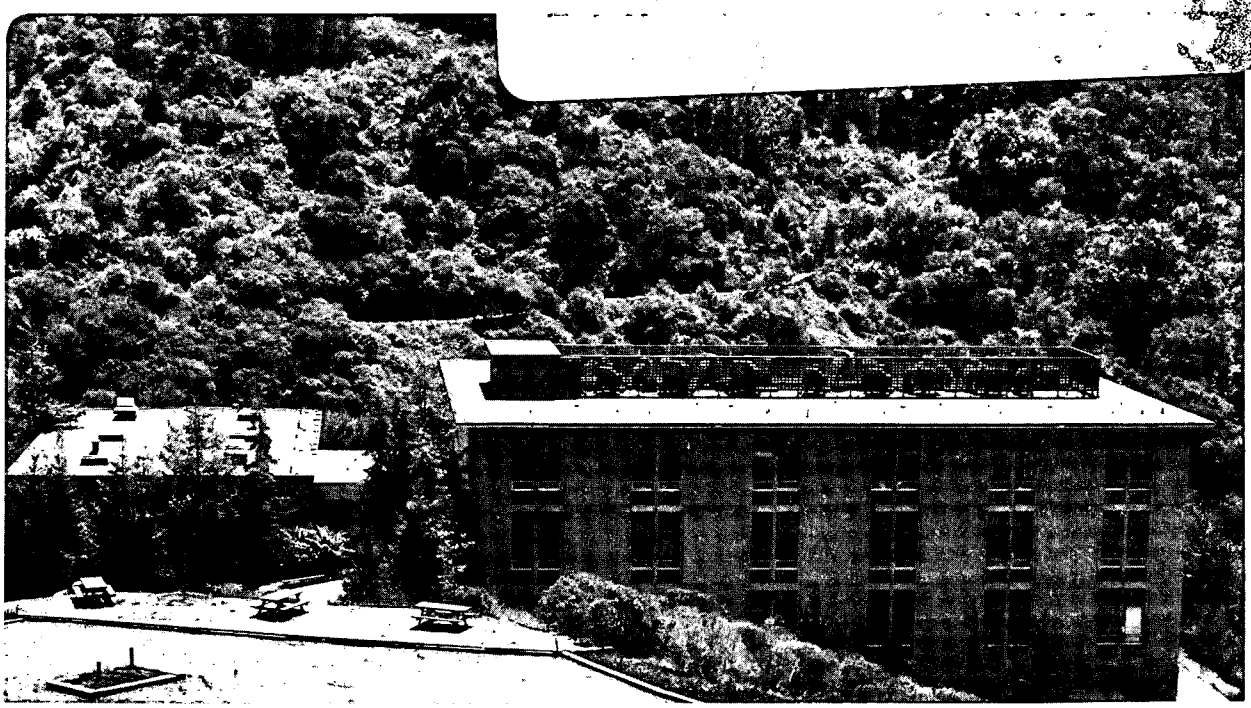

Prepared for the U.S. Department of Energy under Contract DE-AC03-76SF00098

DISCLAIMER

LBL-22035

SPINODAL ORDERING BEYOND THE LIFSHITZ POINT IN Cu_3Pd OBSERVED BY HIGH-VOLTAGE ELECTRON MICROSCOPY

by

S. Takeda*, J. Kulik** and D. de Fontaine***

Materials and Molecular Research Division
Lawrence Berkeley Laboratory
Berkely, CA 94720

*Permanent Address: Department of Physics, College of General Education, Osaka University, Toyonaka, Osaka 560, Japan

**University of California
Department of Physics
Berkeley, Ca 94720

***University of California
Department of Materials Science and Mineral Engineering
Berkeley, CA 94720

August 1986

This work was supported by the Director, Office of Energy Research, Office of Basic Energy Sciences, Materials Sciences Division of the U.S. Department of Energy under Contract No. DE-AC03-76SF00098.

SPINODAL ORDERING BEYOND THE LIFSHITZ POINT IN Cu_3Pd OBSERVED BY HIGH-VOLTAGE ELECTRON MICROSCOPY

by

S. Takeda*, J. Kulik** and D. de Fontaine***

Materials and Molecular Research Division
Lawrence Berkeley Laboratory
Berkely, CA 94720

*Permanent Address: Department of Physics, College of General Education, Osaka University, Toyonaka, Osaka 560, Japan

**University of California
Department of Physics
Berkeley, Ca 94720

***University of California
Department of Materials Science and Mineral Engineering
Berkeley, CA 94720

ABSTRACT

Cu-Pd samples of compositions varying from 16 to 26 at.% Pd were irradiated *in situ* in the 1.5 MeV electron microscope at various temperatures. Low-temperature (-180°C) irradiation produced completely disordered solid solutions, room-temperature irradiation produced steady-state short-range order (SRO), and high-temperature irradiation tended to produce the expected equilibrium long-range order. In particular, the 18 and 20% samples irradiated at room temperature exhibited steady-state modulated SRO although only the simple $L1_2$ ordered structure was expected at equilibrium. It is suggested that spinodal ordering is responsible for these effects. An fcc-based Cu-Pd phase diagram is proposed incorporating ordering stability loci and a metastable Lifshitz point.

This work was supported by the Director, Office of Energy Research, Office of Basic Energy Sciences, Materials Sciences Division of the U.S. Department of Energy under Contract No. DE-AC03-76SF00098.

1. INTRODUCTION

It is well known that, below 500°C, Cu-Pd fcc solid solutions undergo ordering reactions in the range of about 10 to 30 at.% Pd. Evidence has come from X-ray diffraction[1-5], and electron diffraction and microscopy[5-9]. From these and other data, Subramanian and Laughlin[10] proposed an *assessed phase diagram*, of which Fig. 1 is a slightly modified version. The modifications were introduced in order to attempt to incorporate the very recent results of Broddin et al.[11] Much of this diagram is of speculative nature, as no firm evidence for the peritectoid reactions exist. Nevertheless, certain basic features are well established: It is seen that the phase region (α') of the simple ordered structure $L1_2$ peaks not at the expected stoichiometric composition of 25%, but at around 15% Pd. Near stoichiometry, one-dimensional long-period superstructures (LPS) (α_1 region) are found, being replaced at higher Pd content (α_2 region) by two-dimensional LPS. The surprising recent observation[11] that at still higher Pd content the 1-Dim. LPS reappear could not be reconciled with suggested phase boundaries of the diagram of Fig. 1; the two open circles shown on the diagram indicate the presence of 1-Dim. LPS according to Ref. 11. Clearly, in that region, the 1-Dim. LPS may well be metastable with respect to 2-Dim. LPS, and both one- and two-Dim. LPS are certainly metastable with respect to the stable $\alpha_2+\beta'$ equilibrium, β' representing a (B2) bcc superstructure. Stable B2-related equilibria are indicated by light lines in Fig. 1. The dashed lines are *ordering spinodals*, to be discussed later on.

Lately, there has been a regain of interest in long-period superstructures, or periodic antiphase structures since it was suggested[12-15] that the so-called axial next nearest neighbor Ising (ANNNI) model could serve as a simple

theoretical paradigm for LPS systems. The earlier explanation by Sato and Toth[16] for the stability of LPS, based on Fermi surface considerations, is certainly valid, but inadequate for explaining the thermodynamics of LPS stability. The ANNNI model, in its original form[17,18], makes some drastic oversimplifying assumptions, for the sake of convenience, but does predict remarkably well the sequence of polytypes encountered, for example, in Al_3Ti[14] and Ag_3Mg[19] systems. For such alloys, it appeared that, in agreement with the ANNNI model, the LPS could be regarded as generated by a square wave modulation[20] of the $L1_2$ structures, as originally proposed by Fujiwara[21].

In Cu-Au and Cu-Pd LPS, however, well-defined polytypes cannot be readily observed, apparently due to the diffuse or wavy nature of the antiphase boundaries. For such systems, the Jehanno and Pério[22] model (smooth-profile modulating wave) appeared to be more applicable. Thus, it was suggested that two basic types of LPS systems existed: those with sharp antiphase boundaries, of Al_3Ti or Ag_3Mg type, to which the ANNNI model applied, and those with diffuse antiphase boundaries, of Cu-Au or Cu_3Pd types, which were "Fermi surface driven." First-principles calculations of LPS modulation half-wavelength M in Cu_3Pd performed by Györffy and Stocks[23] certainly have given the original Sato ideas a firm quantitative basis.

It can be argued, however, that the Fermi surface effects and ANNNI model description are but complementary aspects of the problem: the electronic energy lowering due to new Brillouin Zone boundaries touching the Fermi surface provide explanations for the existence and magnitude of effective long-range interactions in the alloy, while the ANNNI model, in a generalized form, shows how to handle long-range interactions in a statistical thermodynamics framework, and makes definite statements about expected polytype structures[18] and phase diagrams[17,24,25]. The distinction between

"sharp" and "wavy" classes of systems is perhaps illusory; as mentioned elsewhere[15], the two may simply lie on either side of a commensurate / incommensurate transition.

It is true that such a transition has not been detected as a function of temperature in any experimental system to date. That may be because actual alloys offer too small "experimental windows;" thus, Ag_3Mg, say, seen through the available window, presents only locked-in polytypes, and Cu_3Pd only continuous modulations. In that respect, the recent observation by Broddin et al.[11] is of particular interest: these authors report that antiphase boundaries in Cu_3Pd become quite sharp when the Pd content is high, around 30 at.%, whereas the antiphase boundaries are distinctly wavy at lower concentrations.

The present authors attempted to extend the "experimental window" to lower temperatures in near-stoichiometric Cu_3Pd in the hope of producing sharp antiphase boundaries, hence well-defined polytype structures, below the postulated incommensurate/commensurate boundary. For that purpose, *in situ* electron irradiation in the 1.5 MeV. electron microscope was performed in order to accelerate the low-temperature kinetics. Polytypes were not obtained; instead, modulated short-range order (SRO) was produced in regions of the phase diagram where only the simple $L1_2$ structure was stable. The description of this new phenomenon and its qualitative explanation is the object of the present communication.

2. EXPERIMENTAL RESULTS

2.1 *Samples preparation*

Alloy of 16, 18, 20, 22 and 26 at.% Pd were prepared by arc melting in vacuum from 99.999% pure Cu and 99.997% pure Pd. Ingots were then remelted and splat cooled through the courtesy of L. E. Tanner at the Lawrence

Livermore Laboratory. The purpose of this treatment was to obtain a homogenous solid, with as little coring as possible, and with pronounced <100> texture. Splat cooled foils, which did not have to be rolled, were further homogenized in a sealed quartz tube at 1000°C under one atmosphere of Ar for one day. Solutionized foils were quenched in iced water. Subsequently, 3mm diameter disks were punched out and were jet polished in a methanol solution of 15% HNO_3 at -60°C.

After quenching, specimens were observed in a conventional electron microscope with 100 or 200kV accelerating voltage. Specimens were then transferred to the 1.5 MeV microscope of the National Center for Electron Microscopy (NCEM). Both low and high-temperature double tilting stages were used to provide a total temperature range of -180°C to over 500°C. Diffraction patterns in [001] incidence were taken of all samples in the as-quenched state. Electron irradiation at 1.5MeV was then performed for all samples (except the 18% one) held at -180°C in the miscroscope's cooling stage until completely disordered states were obtained. Electron irradiation was then resumed for up to about 20 min. at room temperature. The heating stage was used to perform *in situ* irridation at temperatures ranging from about 200°C almost up to the disordering temperatures (around 480°C, see Fig. 1). Some diffraction patterns were also taken at temperatures above the ordering transition. The 24% sample was also irradiated at 400keV; the results were similar to those obtained at 1.5 MeV, but kinetics were slower.

2.2 Observations

Consider, for example, the 20% sample, whose diffraction patterns after various treatments are shown in Fig. 2. Analysis of the patterns is given in Fig. 3. The high-temperature pattern (Fig. 2a) is clearly indicative of SRO

fluctuations above the transition temperature. These fluctuations exhibit long wavelength modulations, in agreement with earlier observations[26-28]. The diffraction pattern of the as-quenched condition is shown in Fig. 2b. The specimen was quenched from 1000°C at which temperature no SRO fluctuations are expected to be observable. Apparently a certain amount of spinodal ordering (See Sections 3 and 4, below) occurred during the quench. The intensity pattern in Fig. 2b is similar in character to that of Fig. 2a but with an increase in amplitude and sharpening of the satellites flanking the [100] (and equivalent) positions.

In situ electron irradiation at -180°C completely destroys the SRO, as seen in Fig. 2c. A similar effect was observed previously in the Ni-Mo system by Urban and co-workers[29-31] and by van Tendeloo and Amelinckx[32], and can be interpreted as a "ballistic" effect, in the terminology of Martin[33,34]: random collisions of high-energy incident electrons with Cu or Pd ions tend to create completely disordered states. Indeed, low-temperature high-energy irradiation appears to be the best way to produce truly random solutions, with practically no trace of SRO.

When irradiation is subsequently pursued at room temperature, a most surprising phenomenon is observed: the modulated SRO state, characteristic of the high-temperature fluctuations, reappears although the temperature of about 20°C and the concentration of 20 at.% Pd places the specimen squarely in the region of the phase diagram where the simple, *unmodulated* $L1_2$ ordered structure is stable (phase field α' in Fig. 1). This unexpected modulated SRO state, resulting from the room-temperature irradiation, is surely not the equilibrium state, nor is it a transient: prolonged irradiation at 20°C only produced some sharpening of the satellites accompanied by slight inward motion (see Fig. 4), i.e. by a slight increase in modulation wavelength. Hence,

the system appears to be settling asymptotically into a steady-state condition. Previous studies of CuPd under electron irradiation have been performed only on specimens very close to the stoichiometric composition of 25%Pd. Prolonged irradiation at room temperature actually produced the long range ordered one-dimensional LPS as expected from the phase diagram.[32,35,36]

Irradiation performed at 200°C yields qualitatively the same modulated SRO patterns which evolve with irradiation time in the manner indicatd in Fig. 6: at this temperature, the satellite spacing (proportional to reciprocal modulations wavelength) tends to reach an asymptotic value after about 6 min. At higher temperatures, though, the situation is altered. Irradiaton at 340°C produces a mixed state: since intenstiy is now located at the superstructure positions, some long-range order (LRO) must be present, according to the analysis given in Fig. 3. The evolution in time of the mixed SRO-LRO state is shown in Fig. 7. After irradiation at -180°C produced the completely disordered state, the temperature was increased to 340°C (Fig. 7a) where weak SRO intensity appears even before irradiation is begun. After 10 sec. of irradiation only SRO is present (Fig. 7b) although the intensity has increased dramatically. The central spot, characteristic of LRO, appears after prolonged irradiation (Fig. 7c). Note that, according to the phase diagram (Fig. 1), prolonged heating at 340°C without irradiation should result in the simple $L1_2$ structure, hence the satellites observed in Fig. 7 must be indicative of SRO.

At higher temperatures still, normal kinetics dominate the ballistic effects so that near-equilibrium is reached rather rapidly although the sequence SRO→LRO is qualitatively the same as was observed at 340°C. For example, at 465°C, the 20% sample has a diffraction pattern (Fig. 8c) indicative of three <100> variants of one-dimensional LPS diffracting together (se Fig. 3e), as expected from the equilibrium phase diagram. Figure 8 shows the evolution in

time of the diffraction pattern: satellite peaks are seen to move away from the central superstructure position, indicating that the steady state LRO wavelength at 456°C is less than that characteristic of the 340°C steady-state, which was the starting condition for this experiment. This last conclusion is valid provided that the intense, localized electron beam has not induced any significant change in local composition which might result in a change of wavelength.[34]

Having examined the time evolution of the 20% sample at various temperatures, let us now investigate steady-state diffraction patterns at various temperatures for the other concentrations: 16, 18, 22 and 26%. For the 16% sample, the diffraction pattern taken *in situ* at 500°C shows very weak diffuse intensity due to SRO fluctuations centered at <110> (and equivalent). It is very difficult to detect any splitting into satellite reflections; if satellites are present, their separation distance must be very small, as may be inferred by extrapolating the data of Ohshima and Watanabe[28] or the calculated values of Györffy and Stocks[23]. Likewise, it was not possible to detect any splitting of diffraction maxima in the as-quenched sample. After prolonged irradiation at 20°C, however, (Fig. 9a), the <110> spots are sufficiently intense and spherical in shape that one may affirm that no long wavelength modulation is present. The same conclusion holds at 250°C and at 400°C where the intensity of the superlattice peaks has now increased significantly.

For the 18% sample, the situation, as expected, is intermediate between the 16 and 20% compositions. *In situ* and quenched-in fluctuation SRO patterns show diffuse intensity maxima which no longer have spherical shape. Prolonged irradiation at 20°C and 200°C produces patterns in which the non-sphericity is even more apparent (Fig. 10a). At 360°C (Fig. 10b) however,

sharp superstructure peaks are seen, indicative of unmodulated LRO, i.e. the equilibrium $L1_2$ structure. Irradiation at 465°C produces what appears to be a mixed LRO-SRO state with sharp spots at [100] and equivalent positions accompanied by weak and somewhat diffuse satellites. Irradiation at 485°C produces the equilibrium 1-Dim. LPS LRO state, as expected from the phase diagram.

For the 22% sample (Fig. 11), the satellites are spaced comfortably apart, and can therefore be resolved easily, even at high temperatures above the ordering transition. Patterns are shown in Fig. 11 for temperatures 20°C, 300°C and 464°C. Low temperature irradiation (20°C, 200°C) produces modulated SRO, and the high-temperature treatment produces modulated LRO, with mixed states in between.

Again, the same tendencies are manifest in the 26% sample, although now the satellite spacing is quite large. The patterns remain surprisingly diffuse (Fig. 12), over a wide range of temperatures, almost up to the disordering transition temperature, as if the mixed state occurred over wider temperature intervals in Pd-rich alloys, in comparison to Pd-poor alloys. No evidence of 2-Dim. LPS was found in irradiated samples. Presumably, the *in situ* annealing times under irradiation, limited by availability of machine time, were insufficient to nucleate the 2-Dim. LPS phases.

3. THEORY

3.1. Kinetic consideration

The effect of electron bombardment on order in alloys has been investigated previously[29-32,35,36,38], and the experimental observations are reasonably well understood, at least in a semi-quantitative manner. It is quite

clear that incident high-energy electrons produce random atomic interchanges tending to create complete disorder. This effect of the incident electrons has been termed the *ballistic* one by Martin[33,34]. Additionally, high-energy bombardment tends to create excess vacancies which enhance normal atomic kinetics, thus tending to promote ordering at temperatures for which kinetics would be normally too sluggish.

Some of the results presented here can certainly be understood on the basis of the competition between the ordering and disordering effects of the irradiation: at very low temperatures (-180°), the ballistic term dominates the kinetics completely, and the resulting steady-state condition is that of complete disorder, as described in the previous section. At intermediate temperatures (20°C, 200°C), atomic mobility, enhanced by excess vacancy production (tending to recreate order) and ballistic disordering operate on roughly the same time scales, and are thus competing mechanisms. The fact that SRO, rather than the expected LRO, is created is an interesting effect which has been successfully explained by Urban and co-workers[29-31] on the basis of *spinodal ordering* theory, originally developed for rapidly quenched ordering systems[39]. The theory will be briefly recalled in the next Section but in essence, since the ballistic term tends to destroy order as it is formed, only small-amplitude concentration waves are allowed to exist in the solution, so that, initially, the system evolves towards the thermodynamic state which minimizes the second-order term in the free energy expansion, which in turn governs SRO, LRO being governed by the full free energy functional.

As the irradiation temperature is increased, ordering becomes increasingly competitive since normal kinetics are greatly enhanced (300°C-400°C). At still higher temperatures, the ballistic effect is no match for the rapid normal kinetics, and LRO results (~450°).

It is planned, in future, to apply a modified form of Martin's model to modulated SRO. For the present, however, let us apply a quasi-equilibrium model to explain the steady-state morphologies described in Sect. 2.

3.2. Spinodal Ordering

Spinodal ordering theory[39,40] is based on the concentration wave idea initially proposed by Landau and Lifshitz[41], Krivoglaz[42] and Khachaturyan[43]: the configurational free energy is expanded in powers of local concentration deviations

$$\gamma(p) = c(p) - \bar{c}$$

where c(p) is a suitably averaged concentration at lattice point p, and $\bar{c}$ is the overall average concentration in the binary solid solution. The free energy funtional takes the form

$$F(\gamma(p_1), \gamma(p_2)\ldots\gamma(p_N)) = F_0 + F_1 + F_2 + F_3 + \ldots,$$

N being the number of lattice sites, with expansion terms given by

$$F_n = \frac{1}{n!} \left[\sum_p \gamma(p) \frac{\partial}{\partial\gamma(p)}\right]_o^n F \quad , \qquad (1)$$

the subscript o indicating that derivatives must be evaluated in the disordered state. At equilibrium, the first-order (F_1) term vanishes, so that the difference ΔF between the free energies of states containing concentration fluctuations (γ) and the completely disordered state (all γ=0) is given by

$$\Delta F \equiv F - F_0 = F_2 + F_3 + F_4 + \ldots \qquad (2)$$

In the Fourier respresentation, successive terms of the Landau expansion are given by

$$F_2 = \frac{N}{2} \sum_h F''(h) \, |\Gamma_h|^2 \qquad (3)$$

$$F_3 = \frac{N}{3!} \sum_{h} \sum_{h'} \sum_{h''} F'''(h,h',h'') \times \Gamma(h)\Gamma(h')\Gamma(h'')\ \delta(h+h'+h''-g) \qquad (4)$$

etc. In these equations, Γ are the Fourier tranforms of the γ, i.e. they are amplitudes of concentration waves, of wave vector $\mathbf{k}(h)$, h being a suitable index in reciprocal space. F" and F"' denote Fourier transforms of second and third derivatives (etc.) as per Eq. (1). The Kronecker delta in Eq. (4) equals unity if the three wave indices sum to a reciprocal lattice vector $\mathbf{k}(g)$, zero otherwise.

Just below a second-order transition, the amplitudes $|\Gamma|$ are vanishingly small, hence, the F_2 (harmonic term) dominates the free energy expansion. Thus, according to the Landau theory, the transition occurs when F" changes sign for that particular *ordering wave* h^o which gives F" its minimum value. The locus of a second-order transition in (c,T) phase diagram space is thus

$$F''(h^o;c,T) = 0 \qquad (5)$$

which defines a critical temperature T_o for every concentration c.

At a first-order transition T_t, one or more concentration waves combine to give negative contributions to the anharmonic terms F_3, F_4... in the Landau expansion, thereby allowing ΔF to vanish for $T_t > T_o$. The latter temperature T_o, defined by Eq. (5), now represents an *instability*, or spinodal ordering temperature, below which ordering waves h^o are spontaneously amplified[39,40]. Thus, upon rapid quenching from the solid solution state to below the instability temperature T_o, concentration waves of wave vectors in the vicinity of h^o grow in amplitude before the true equilibrium LRO state has a chance to nucleate: as long as wave amplitudes $|\Gamma|$ remain small, the F_2 terms dominate and the state of order to which the system will tend is that which minimizes F", rather than the free energy itself. Concentration waves which minimize F"

are also those which maximize the SRO fluctuation intensity at high temperature since, by application of the fluctuation-dissipation theorem one has[40]

$$I_{SRO}(h) \propto k_B T/F''(h) \qquad (6)$$

where k_B is Boltzmann's constant. The Krivoglaz[42] and Clapp and Moss[44] model can then be recovered from Eq. (6) by using a Bragg-Williams formula for the free energy F.

It therefore follows that rapid quenching may yield SRO states which are slightly amplified versions of the high-temperature equilibrium fluctuation state, which may also be looked upon as an arrested transient state into which the system may be frozen on its way to equilibrium LRO. Such is the phenomenon of spinodal ordering which is of course particularly apparent when the set of wave vectors which produce SRO are different from that which produces LRO. Such is the case in Ni-Mo, for example, as described elsewhere[39,45].

Irradiation can produce qualitatively similar effects, as shown by Urban and co-workers[29-31], also in the case of Ni-Mo, and by van Tendeloo and co-workers for several other systems including Cu_3Pd[32,35,36,38]. The resulting low-temperature state is then no longer an "arrested transient," but a steady state irradiated condition. Spinodal ordering applies equally well: now the anharmonic terms in F are prevented from taking over by the disordering effect of the ballistic term which limits the growth of the wave amplitudes $|\Gamma|$. It was indeed found that, in the low temperature ranges (but not too low) the irradiated steady state condition is characterized by the same wave vectors which characterize both the SRO fluctations seen above the the first-order transition at high temperature and the "arrested" condition at low temperature after rapid quenching.

3.3. Beyond the Lifshitz point

It is well known that any function having crystallographic symmetry, i.e. rotational and translational, must have extrema at *special points* (SP) where rotational symmetry elements intersect a point (Lifshitz criterion[41]). The SP in the first Brillouin zone were determined for all 230 space groups[46]; for fcc crystals these are <000>, <100>, <1½0> and <½½½>. Normally, one expects that F" will be minimized at one of the SP; in that case, the ordering wave h^o will be that of a *symmetry-dictated minimum*. Different solid solutions, in various concentration ranges, can then be classified according to the SP which minimizes F", i.e. according to the SP ordering wave instability. Thus, for example, Cu-Au and Cu-rich Cu-Pd are <100>-instability systems, while Ni-rich Ni-Mo is <1½0>-instability system[47].

It may happen, of course, that F" presents accidental minima away from the SP, specifically at points $\pm q$ away from the SP, along equivalent directions in reciprocal space. If the transitions are second order, then a new kind of critical point must appear, the so-called *Lifshitz point*[48,49]. That point (in phase diagram space) may be defined as follows [49,13]: the Lifshitz point L is a multicritical point which divides a line of second-order transitions into two segments on one of which the equilibrium order parameter is characterized by a fixed wave vector $\mathbf{k}(h^o)$, allowed by the Lifshitz condition (SP), while on the second, $\mathbf{k}(h)$ varies continuously as some parameter (such as concentration) is varied. Point L is also the terminus of a second line which separates the phase diagram into two regions, one along which F" is minimized by wave h^o at a SP, one along which F" is minimized by wave $h=h^o\pm q$ ($q\neq 0$).

In the case of interest here, satellite reflections are located along a line in reciprocal space at positions h10 (and crystallographically equivalent). Any k-space function, in particular F", having required fcc symmetry, can be

expanded in a sum of "shell functions" Φ_s (one for each coordination shell s) as follows[39]:

$$F''(\mathbf{k}) = \sum_s w_s \Phi_s(\mathbf{k}) + \Phi_o \qquad (7)$$

where the w_s are effective interaction parameters, all h-independent terms having been collected into Φ_o. The shell functions, given explicitly elsewhere[39], at h10 take the form:

$$\begin{aligned}\Phi_s(h10) = \frac{z_s}{3}[&\cos 2\pi h p_1(\cos 2\pi p_2 + \cos 2\pi p_3) \\ &+ \cos 2\pi h p_2(\cos 2\pi p_3 + \cos 2\pi p_1) \\ &+ \cos 2\pi h p_3(\cos 2\pi p_1 + \cos 2\pi p_2)]\end{aligned} \qquad (8)$$

where p_1, p_2, p_3 are Miller indices of an arbitrary lattice point in the s^{th} shell, and z_s is the coordination number of the shell. Since, on the fcc lattice, the three p_i's must be either all integers, or one an integer and the two others half-integers, it turns out that only "even cosines," of the form $\cos 2\pi nh$ (n=1,2,...), survive in Eq. (8). When like cosines are grouped in Eq. (7), the following expression results:

$$F''(h10) = \sum_n J_n \cos 2\pi nh + \Phi_o \qquad (9)$$

where the effective *axial* interactions J_n can be expressed as linear combinations of the w_s, defined in Eq. (7). In the Bragg-Williams approximation, the w_s parameters are temperature independent pair interactions, usually denoted by the symbol V_s, hence, in that approximation the J_n are also temperature-independent.

The cosine series (9) has exactly the same form as that for the ANNNI model, so that the derivations given previously[13] can be taken over with no

essential modifications. Thus, it is convenient to expand the harmonic coefficient F" in powers of the difference $q=h-h^o$ about the appropriate SP:

$$F''(h;T,c) = \phi_o + \phi_2 q^2 + \phi_4 q^4 + \ldots \quad , \qquad (10)$$

In this equation, odd derivatives ϕ do not appear since they must vanish by symmetry at the SP h^o about which they are evaluated.

It was shown elsewhere[13] that, usually, ϕ_4 must be positive, so that, sufficiently close to point L, the expansion (10) may be limited to fourth order in q. Minima of F" are then located at $q_{min}=0$ and at

$$q_{min} = \pm \sqrt{(-\phi_2/2\phi_4)} \quad , \qquad (11)$$

the second solution being valid for $\phi_2<0$. Inserting q_{min} into (10) yields

$$\phi_{min}(T,c) = \begin{cases} \phi_o & \text{for } \phi_2>0 \\ \phi_o - \frac{1}{4}\frac{\phi_2^2}{\phi_4} & \text{for } \phi_2<0 \end{cases} \quad . \qquad (12)$$

Hence, second-order transition lines on either side of L are given by (T,c) loci $\phi_2=0$ (SP ordering), and $\phi_2^2 - 4\phi_o\phi_4 = 0$ (non-SP ordering), which are the two possibilities for $\phi_{min}(T,c)=0$. Thus the Lifshitz point has coordinates defined by

$$\phi_o(T_L,c_L) = \phi_2(T_L,c_L) = 0 \quad , \qquad (13)$$

at the intersection of the SP-ordering line and the SP/non-SP separation line.

These results, concerning the location of transition lines and Lifshitz point, were derived originally for second-order transitions. In the present case, symmetry requires that all transitions be first-order so that all conclusions based upon analysis of the harmonic term only necessarily pertain to metastable states, obtained by supressing the first-order transitions. Hence, loci $\phi_o=0$, $\phi_{min}=0$, must represent stability limits, rather than true

equilibrium transitions and, likewise, Eq. (13) must represent a metastable Lifshitz point. Therefore, the present formalism extends "beyond the Lifshitz point" the earlier spinodal ordering formalism, the latter itself being considered as a non-equilibrium extension of the Landau theory of second-order transitions.

It must be emphasized, however, that the location of instability lines cannot be determined rigorously, either theoretically or experimentally: theoretically, the locus of vanishing of second derivations depends on the analytical model adopted for the free energy and experimentally, the temperature at which instability sets in must depend upon past history of the system, unlike equilibrium transitions which are history-independent. Nevertheless, the approximate determination of stability limits can be of considerable help in semi-quantitative analysis of the behavior of either quenched or irradiated solid solutions, as will now be shown.

4. DISCUSSION

The various metastable loci, $\phi_o=0$, $\phi_{min}=0$, $\phi_2=0$, and their intersection L, the metastable Lifshitz point, have been sketched on Fig. 1 in a manner which best accounts for the available experimental data. In particular, line $\phi_2=0$ was placed so that all SP (unmodulated) SRO states, both equilibrium fluctuation and steady-state, are to the left of it, and all non-SP (modulated) SRO states are to the right. If a Bragg-Williams model were used for the free energy, the ϕ_2 line would be straight and vertical; in Fig. 1 it was drawn slightly curved for the following reasons: low-temperature irradiation steady-state SRO appears to be unmodulated (no satellites) for the 16% composition (see Fig. 9a) but modulated for the 18% composition (see Fig. 10a). On the other

hand, although it is not clear from the present high-temperature *in situ* results, extrapolation of the Ohshima and Watanabe data[28], and also first-principles calculations[23] indicate that equilibrium fluctuation SRO becomes "modulated" at lower concentrations, around 13 or 14%. Furthermore, CVM calculations[50] for 2-Dimensional systems clearly yield curved ϕ_2 lines.

The ordering instabilities, $\phi_0=0$ for the SP ordering and $\phi_{min}=0$ for non-SP ordering, have been drawn fairly close to the equilibrium first-order transition lines, particularly ϕ_{min}, because experimental evidence[10] indicates very narrow two-phase regions so that the postulated peritectoids must be close to being critical end points, through which instability lines must pass[51].

In principle, it would be possible to calculate these several loci provided one had (a) reliable free energy models, such as the CVM (b) one knew what interaction parameters V_s to insert. It was argued elsewhere[15], on the basis of early modulation wavelength data, that the ground states for ordering in the Cu-rich Cu-Pd system were $L1_2$ (<∞> in ANNNI model notation) and <3>, the latter representing a structure consisting of three $L1_2$ unit cells followed by three others in antiphase relation to the first ones. A similar conclusion was reached recently by Broddin et al.[11] Thus, according to the formalism leading to Eq. (9), effective axial interaction up to and including J_3 are required. In the fcc lattice, J_3 must include pair interactions out to at least the 17th coordination shell. The simplest, albeit unrealistic scheme, consists in retaining only J_1 and J_3 in the cosine series (9). Then, as shown elsewhere[15], the ANNNI model multiphase point, to which the ϕ_2 line must tend at absolute zero of temperature, must be located at ratio $\kappa \equiv |J_3/J_1| = 1/3$ and the Lifshitz point must be located (in a mean field approximation) at $\kappa=1/9$. Experimental evidence suggests that, in Cu-Pd, κ increases monotonically with Pd content so that the concentration axis can be put into one-to-one correspondence with

ratios of J parameters, in principle. That being the case, the L point must then be located at leaner Pd concentration than the multiphase point, again requiring the ϕ_2 line to curve as indicated in Fig. 1.

Let us now summarize the explanation of the experimental findings: upon quenching from the disordered solution sufficiently rapidly to suppress the first-order transition, spinodal ordering takes place as the instability lines are crossed. Further amplification of ordering waves cannot occur, however, since kinetics at the quenching temperature are too low. The result of the quenching operation is thus an "arrested transient" SRO state, as evidenced by the diffraction pattern of Fig. 2b, for example. Irradiation at very low temperatures (-180°) then destroys all SRO, as explained above, but prolonged irradiation at 20° or 200°C restores the SRO state which now appears in a steady state condition. Whether this steady-state SRO is modulated (satellites) or not will depend upon whether the sample composition, at the irradiation temperature, is to the right or, respectively, to the left of the ϕ_2=0 locus. At these temperatures, then, ϕ_2 must be located around 17 at.% Pd. Satellite spacing clearly increases as the Pd content increases, eventually approaching that of the <3> structure.

At higher temperatures, the metastable loci constructed in Fig. 1 are no longer of great use: the SRO states are now mixed in with LRO, or disappear altogether due to the dominance of normal high-temperature kinetics which restore the equilibrium LRO states. Examination of the interplay between normal diffusion and ballistic effects, required to determine where irradiation SRO leaves off and LRO begins, would necessitate a model of the system's kinetics and is planned for a future study. Here, only a quasi-equilibrium model was presented, but it accounts quite well for the observed pheonomena.

5. CONCLUSION

The expected sharpening of antiphase boundaries under low-temperature electron irradiation did not take place. Instead, a serendipitous discovery was made: it was found that room temperature irradiation of a completely disordered solid solution could produce long-wavelength modulated steady-state SRO for Cu-Pd samples in regions of the phase diagram where only simple $L1_2$ ordering could be found at equilibrium. The authors believe this to be the first observation of its kind ever reported.

This puzzling effect could be explained, at least qualitatively, by applying spinodal ordering ideas to irradiated systems, and by extending the model "beyond the Lifshitz point," i.e. to cases for which the harmonic coefficient F" of the free energy possesses minima away from the Special Points. These generalizations lead to the notion of SP (commensurate) and non-SP (incommensurate) stability limits and of a metastable Lifshitz point.

The experimental portion of this investigation was made possible by use of a high-voltage electron microscope with which it is possible to study, *in situ*, various types of equilibria: (a) high-temperature equilibrium SRO fluctuations, (b) equilibrium LRO at various temperatures, (c) steady-state SRO under irradiation at low temperatures. In each case, both diffraction patterns (reciprocal space) and micrographs (direct space) can be recorded. Thus, far more information concerning thermodynamics of alloys can be obtained than would be available by performing standard equilibrium (phase diagram) studies alone. More quantitatively, SRO studies can lead to knowledge of effective pair interactions, V_s, which govern the fundamentals of ordering processes.

ACKNOWLEDGEMENTS

The authors are grateful to Drs. A. Finel, P. Turchi and G. M. Stocks for helpful conversations. TEM work was performed on the 1.5 MeV microscope at the National Center for Electron Microscopy, Lawrence Berkeley Lab. The authors are indebted to Dr. K. Westmacott for his support and interest and to D. Ackland for invaluable technical help. One of us (S.T.) benefitted from an MMRD collaborative fellowship. This work was supported by the Director, Office of Energy Research, Office of Basic Energy Sciences, Materials Sciences Division of the U.S. Department of Energy under Contract No. DE-AC03-76SF00098.

REFERENCES

1. K. Schubert, B. Kiefer, M. Wilkens, and R. Haufler, *Z. Metallkd.* **46**, 692 (1955).
2. M. Hirabayashi and S. Ogawa, *J. Phys. Soc. Japan* **12**, 259 (1957).
3. K. Okamura, *J. Phys. Soc. Japan* **28**, 1005 (1970).
4. O. Michikami, H. Iwasaki, and S. Ogawa, *J. Phys. Soc. Japan* **31**, 956 (1971).
5. A. Souter, A. Colson, and J. Hertz, *Mem. Sci. Rev. Met.* **68**, 575 (1971).
6. D. Watanabe and S. Ogawa, *J. Phys. Soc. Japan* **11**, 226 (1956).
7. M. Guymont and D. Gratias, *Phys. Stat. Sol.* **A36**, 329 (1976).
8. M. Guymont, R. Portier, and D. Gratias, *Electron Microscopy and Analysis* 1981, Conf. Ser. No. 61, ed. M. J. Goringe, Inst. Phys. Bristol and London, 387 (1981).
9. O. Terasaki and D. Watanabe, *Jpn. J. Appl. Phys.* **20**, L381 (1981).
10. P. R. Subramanian and D. E. Laughlin, to appear in *Bulletin of Alloy Phase Diagrams.*
11. D. Broddin, G. van Tendeloo, J. Van Landuyt, S. Amelinckx, R. Portier, M. Guymont and A. Loiseau, *to be published.*
12. J. Kulik and D. de Fontaine in *Phase Transformations in Solids, Materials Research Society Symposia Proceedings vol. 21*, T. Tsakalakos, ed., p. 225 (North-Holland, NY, 1984).
13. D. de Fontaine and J. Kulik, *Acta metall.* **33**, 145 (1985).
14. A. Loiseau, G. van Tendeloo, R. Portier and F. Ducastelle, *J. de Physique* **46**, 595 (1985).

15. D. de Fontaine, A. Finel, S. Takeda and J. Kulik, in *Noble Metal Alloys*, T. B. Massalski, W. B. Pearson, L. H. Benett and Y. A. Change, eds., The Met. Soc. of AIME, pp. 49-62 (1986).

16. H. Sato and R. S. Toth, in *Alloying Behavior and Effects in Concentrated Solid Solutions*, T. B. Massalski, ed., 295, Gordon and Breach, NY (1965).

17. P. Bak and J. von Boehm, *Phys. Rev.* **B21**, 5297 (1980).

18. M. E. Fisher and W. Selke, *Phil. Trans. Royal Soc. London*, **A302**, 1 (1981).

19. J. Kulik, S. Takeda and D. de Fontaine, *to be published.*

20. D. de Fontaine, *J. Phys.* **A17**, L713 (1984).

21. K. Fujiwara, *J. Phys. Soc. Japan* 12, 7 (1957).

22. G. Jehanno and P. Pério, *J. de Physique*, **25**, 966 (1964).

23. B. L. Gyorffy and G. M. Stocks, *Phys. Rev. Letters* **50**, 374 (1983).

24. P. M. Duxbury and W. Selke, *J. Phys.* **A16**, L741 (1983).

25. W. Selke and P. M. Duxbury, *Z. Phys.* **B57**, 49 (1984).

26. D. Watanabe, *J. Phys. Soc. Japan*, 14, 436 (1959).

27. K. Ohshima, D. Watanabe and J. Harada, *Acta Crystallogr.* **A32**, 883 (1976).

28. K. Ohshima and D. Watanabe, *Acta Crystallogr* **A29**, 520 (1973).

29. S. Banerjee, K. Urban and M. Wilkens, *Acta metall.* **32**, 299 (1984).

30. S. Banerjee and K. Urban, *Phys. Stat. Sol.* (a) **81**, 145 (1984).

31. J. Mayer and K. Urban *(submitted to Acta metall.)*.

32. G. van Tendeloo and S. Amelinckx, *Journal de microscopie et de spectroscopie électroniques* **6**, 371 (1981).

33. G. Martin, *Phys. Rev.* **B30**, 1424 (1984).

34. P. Bellon and G. Martin *(to be published)*.

35. G. van Tendeloo, J. van Landuzt and S. Amelinckx, *Rad. Effects* **41**, 179 (1979).

36. G. van Tendeloo, J. van Landuzt and S. Amelinckx in *Electron Microscopy 1980,* Volume 4, p. 266, Congress Foundation, Leiden, 1980.

37. P. R. Okamoto and N. Q. Lam, *Mat. Res. Soc. Symposium Proceedings* **41**, 241 (1985).

38. G. van Tendeloo, R. de Ridder and S. Amelinckx in *Electron Microscopy 1980,* Volume 4, p. 270, Congress Foundation, Leiden, 1980.

39. D. de Fontaine, *Acta metall.* **23**, 553 (1975).

40. D. de Fontaine, *Solid State Physics* **34**, 73 (1979).

41. L. D. Landau and E. M. Lifshitz, *Statistical Physics*, p. 366, Addison-Wesley, Reading, MA (1958).

42. M. A. Krivoglaz, *The Theory of X-ray and Thermal Neutron Scattering from Real Crystals,* New York, Plenum (1969).

43. A. G. Khachaturyan, *Phys. Stat. Sol. (6)* **60**, 9 (1973).

44. P. C. Clapp and S. C. Moss, *Phys. Rev.* **142**, 418 (1966).

45. G. van Tendeloo, S. Amelinckx and D. de Fontaine, *Acta crystallogr.* **B41**, 281 (1985).

46. J. M. Sanchez, D. Gratias and D. de Fontaine, *Acta crystallogr.* **A38**, 214 (1982).

47. T. Mohri, J. M. Sanchez and D. de Fontaine, *Acta metall.* **33**, 1171 (1985).

48. C. Haas, *Phys. Rev.* **A140**, 863 (1965).

49. R. M. Hornreich, M. Luban and S. Shtrikman, *Phys. Rev.* **B19**, 3799 (1979).

50. A. Finel and D. de Fontaine, *J. Stat. Physics* **43**, 645 (1986).

51. S. M. Allen and J. W. Cahn, in *Alloy Phase Diagrams*, L. H. Bennett, T. B. Massalski, B. C. Giessen, eds., North Holland, pp. 195-210, 1983.

FIGURE CAPTIONS

Figure 1. Cu rich side of the Cu-Pd phase diagram. Heavy solid lines indicate equilibria between the fcc solid solution (α) and the fcc-derived ordered phases: $L1_2$ (α'), 1-dimensional LPS (α_1) and 2-dimensional LPS (α_2). Light solid lines indicate equilibria between the ordered bcc phase (β') and the α and α_2 phases. The point L is a metastable Lifshitz point. The loci $\phi_0=0$, $\phi_{min}=0$ and $\phi_2=0$ shown by dashed or dotted lines are discussed in the text. The two open circles in the $\alpha_2+\beta'$ two phase region are points where Broddin et al.[11] observed a (metastable?) 1-dimensional LPS.

Figure 2. Cu 20 at. % Pd: a) equilibrium SRO fluctuations *in situ* at 535°C, b) as quenched from 1000°C, c) after irradiation at -180°C, d) result of room temperature irradiation of the disordered state shown in (c).

Figure 3. Schematic of diffraction patterns seen in CuPd. Patterns (a), (b) and (c) show the 3 possible variants of the 1-dimensional LPS which are, respectively, modulation along [100], [010], and [001]. Pattern (d) is a combination of (a) and (b), while (e) is a combination of all three variants. Pattern (f) is indicative of SRO. Note the absence of intensity at [100] and equivalent positions in (f).

Figure 4. Cu 20 at. % Pd: a) reappearance of SRO at room temperature after complete disorder was produced at -180°C, b) after 185 sec. of irradiation at room temperature, c) after 720 sec. of irradiation at room temperature.

Figure 5. Distance q in reciprocal space of the intensity maxima from the [100] position as a function of irradiation time at 200°C. The unit distance in reciprocal space is taken as [100].

Figure 6. Cu 20 at. % Pd at 340°C: a) appearance of weak SRO intensity at 340°C after initial irradiation at -180°C had produced complete disorder, b) after 10 sec. of irradiation at 340°C, c) after 1440 sec. of irradiation.

Figure 7. Cu 20 at. % Pd at 456°C: a) initial state at 456°C after annealing for 1 hour at 340°C, note the sharpness of the satellites despite the absence of the [100] spot, b) appearance of LRO after 30 sec. of irradiation, c) after 720 sec. of irradiation.

Figure 8. Steady states under irradiation in the Cu 16 at. % Pd specimen: a) 20°C, b) 250°C, c) 400°C.

Figure 9. Steady states under irradiation in the Cu 18 at. % Pd specimen: a) 20°C, b) 360°C, c) 465°C, d) 485°C.

Figure 10. Steady states under irradiation in the Cu 22 at. % Pd specimen: a) 20°C, b) 300°C, c) 464°C.

Figure 11. Steady states under irradiation in the Cu 20 at. % Pd specimen: a) 21°C, b) 427°C, c) 466°C.

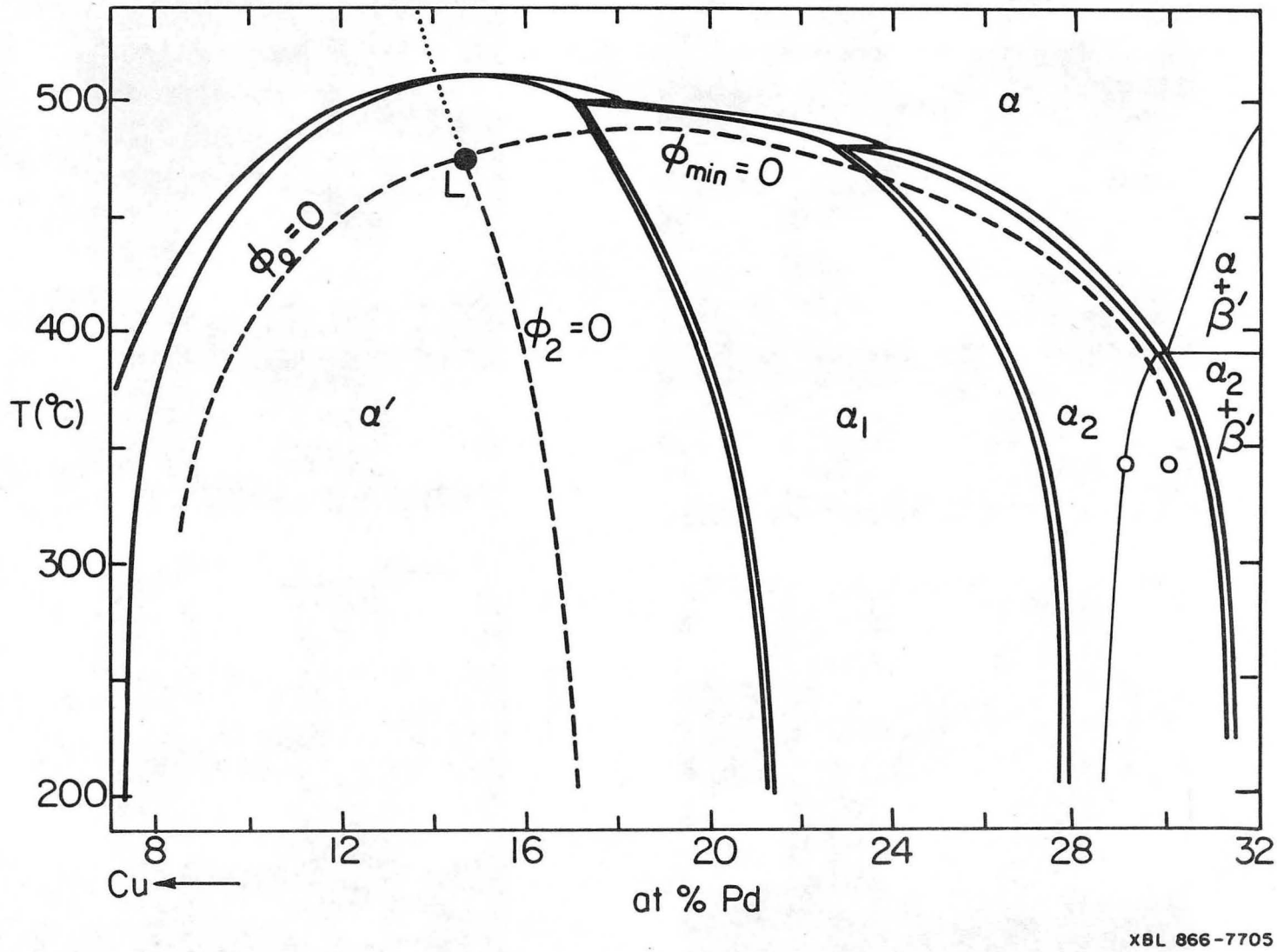
500
400
300
200
T(°C)
8
12
16
20
24
28
32
Cu
at % Pd
α
α'
α1
α2
L
$\phi_{min} = 0$
$\phi_2 = 0$
$\phi_2 = 0$
α + β'
α2 + β'
XBL 866-7705

Fig. 1

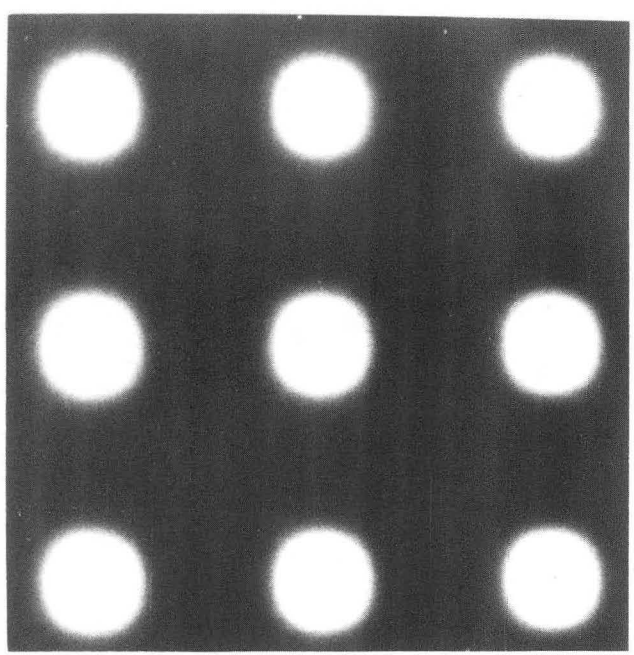

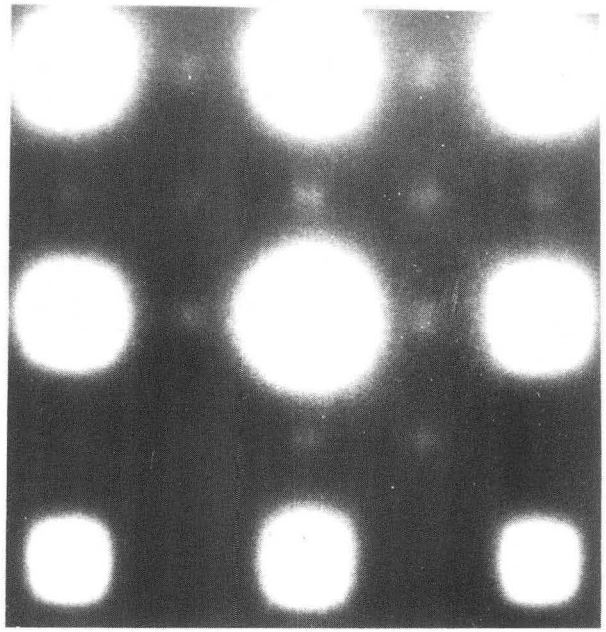

as quenched

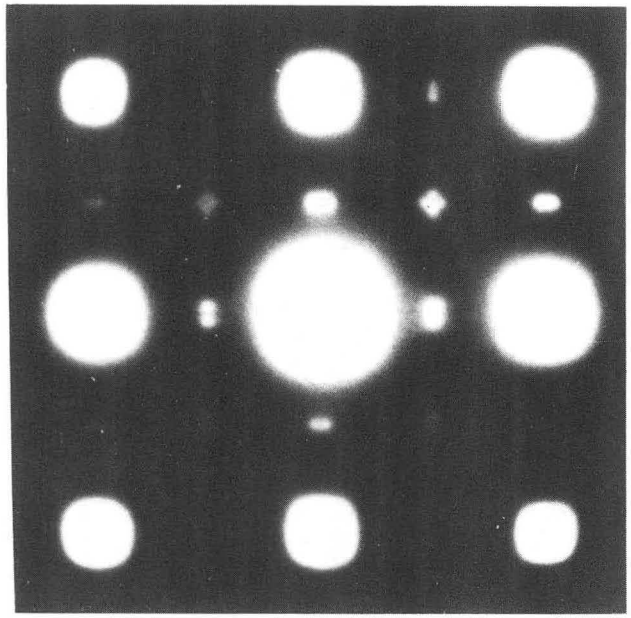

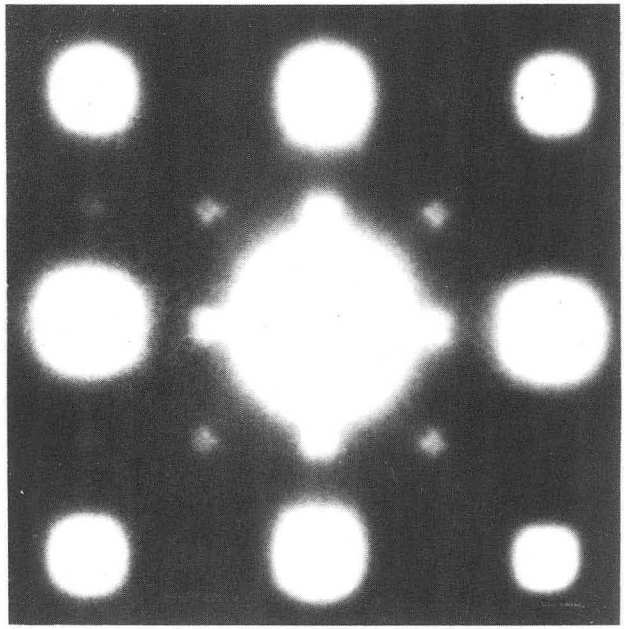

-180°C

R.T.

20%Pd

Fig. 2

XBB 867-5904

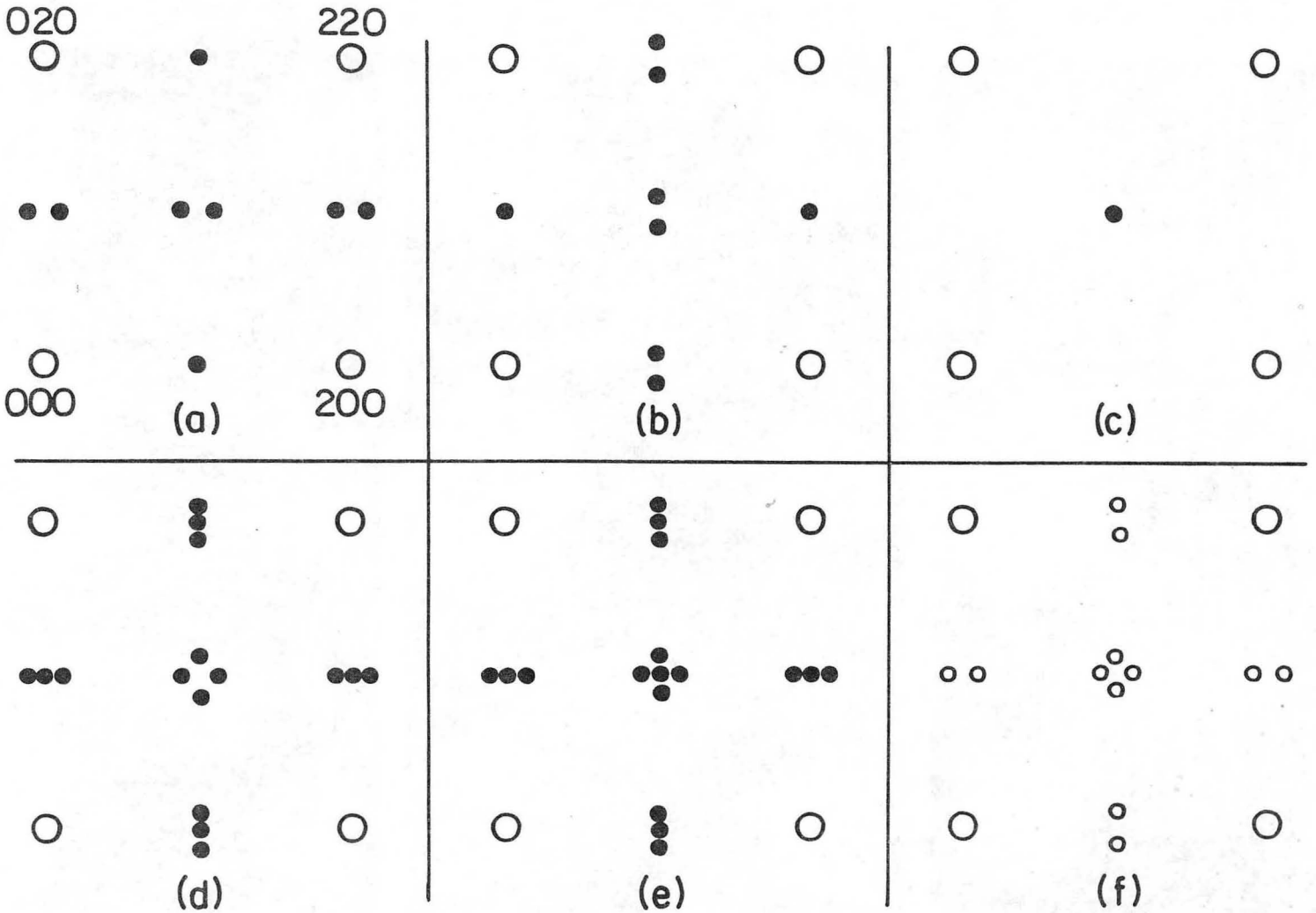

Fig. 3

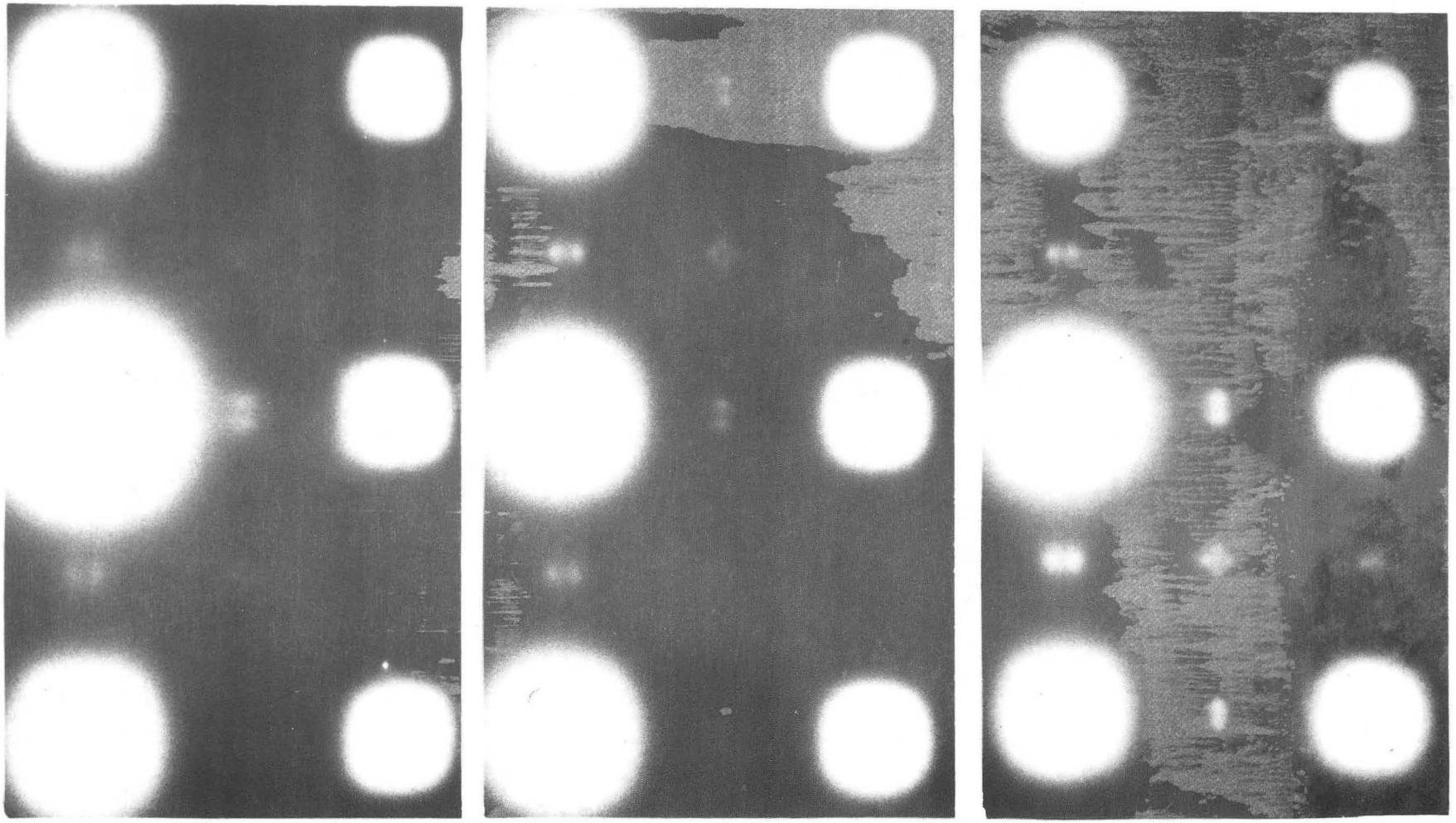

XBB 855-4049

Fig. 4

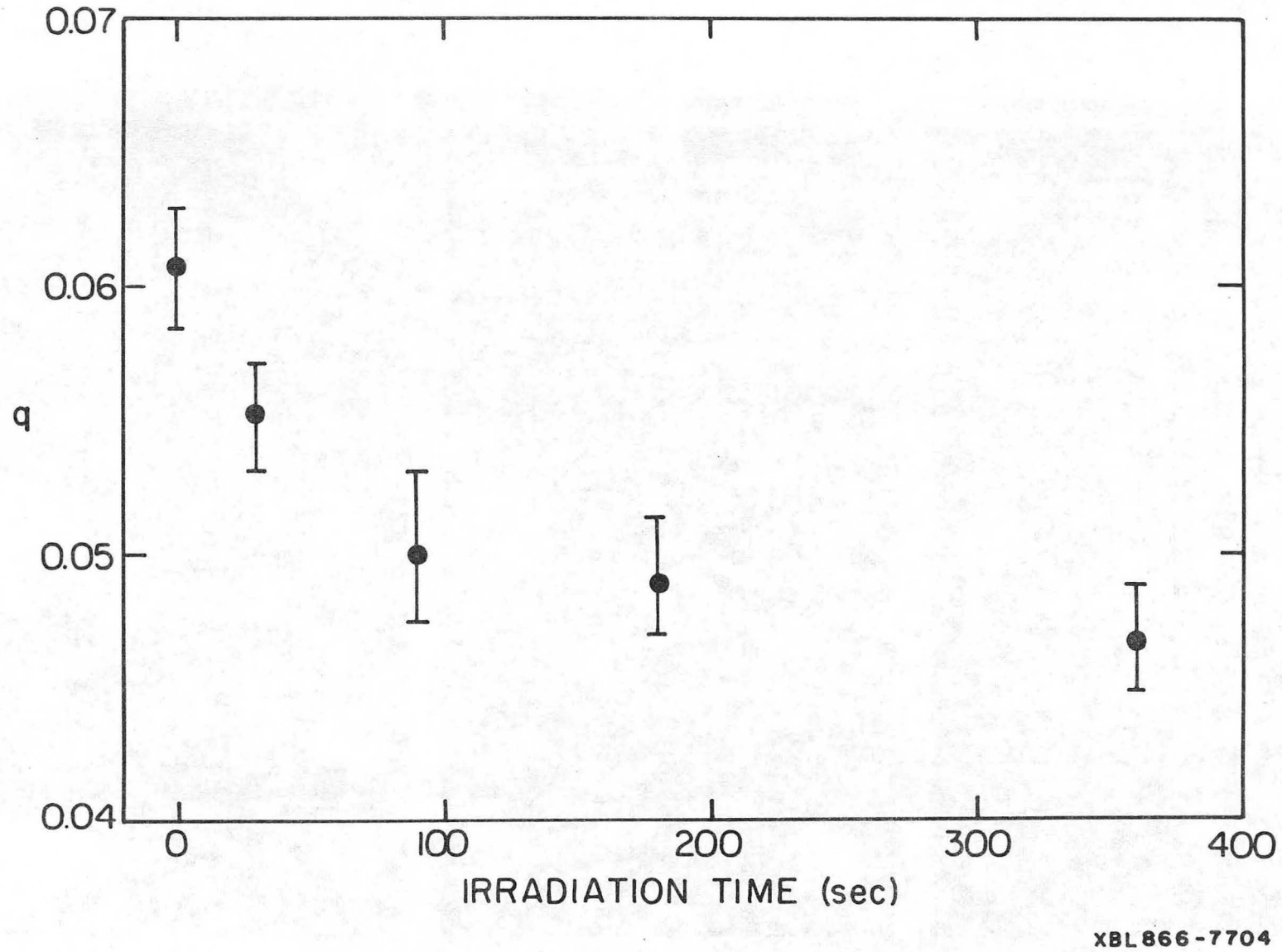
0.07
0.06
0.05
0.04
q
0
100
200
300
400
IRRADIATION TIME (sec)
XBL866-7704

Fig. 5

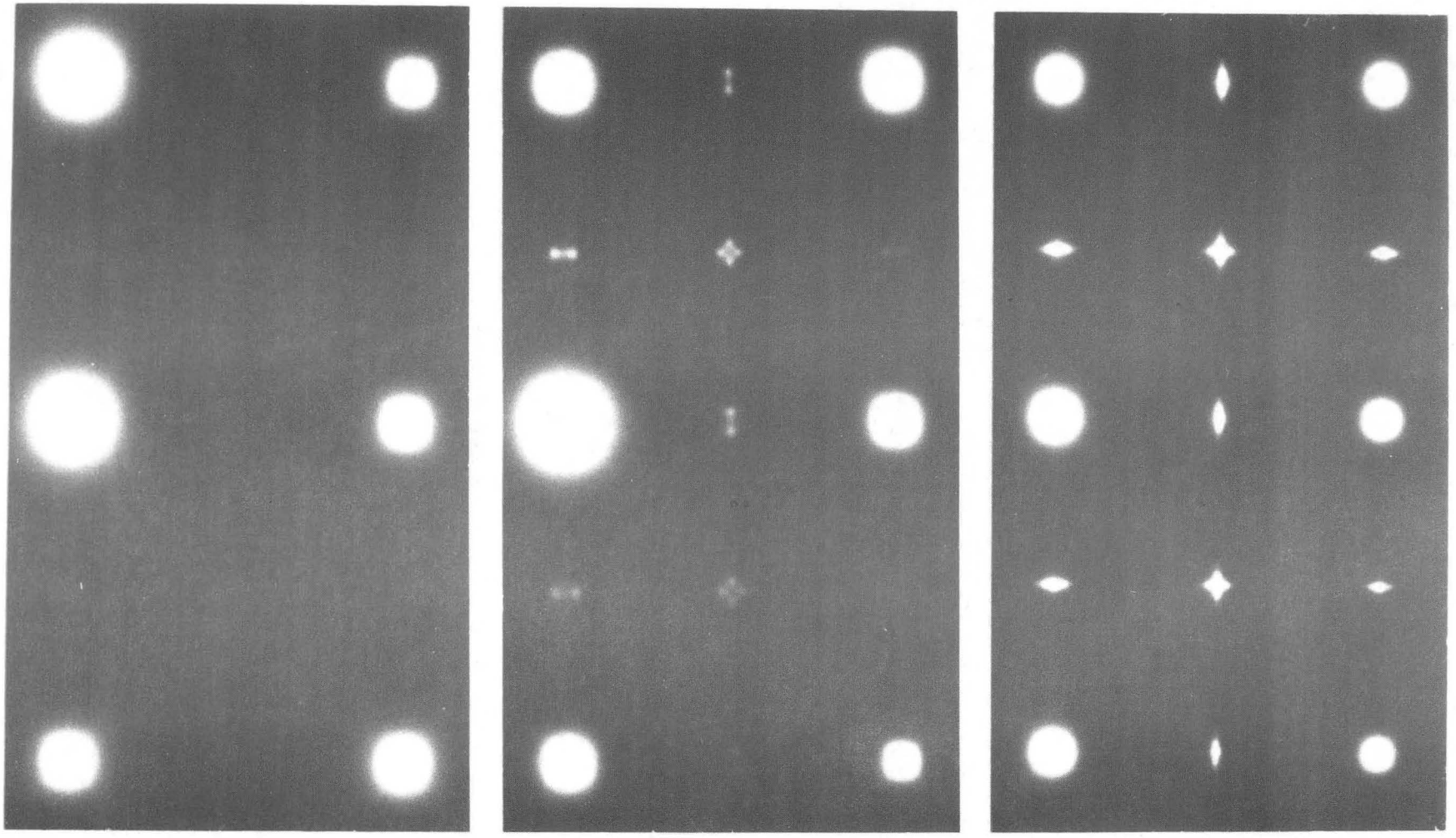

XBB 855-4052

Fig. 6

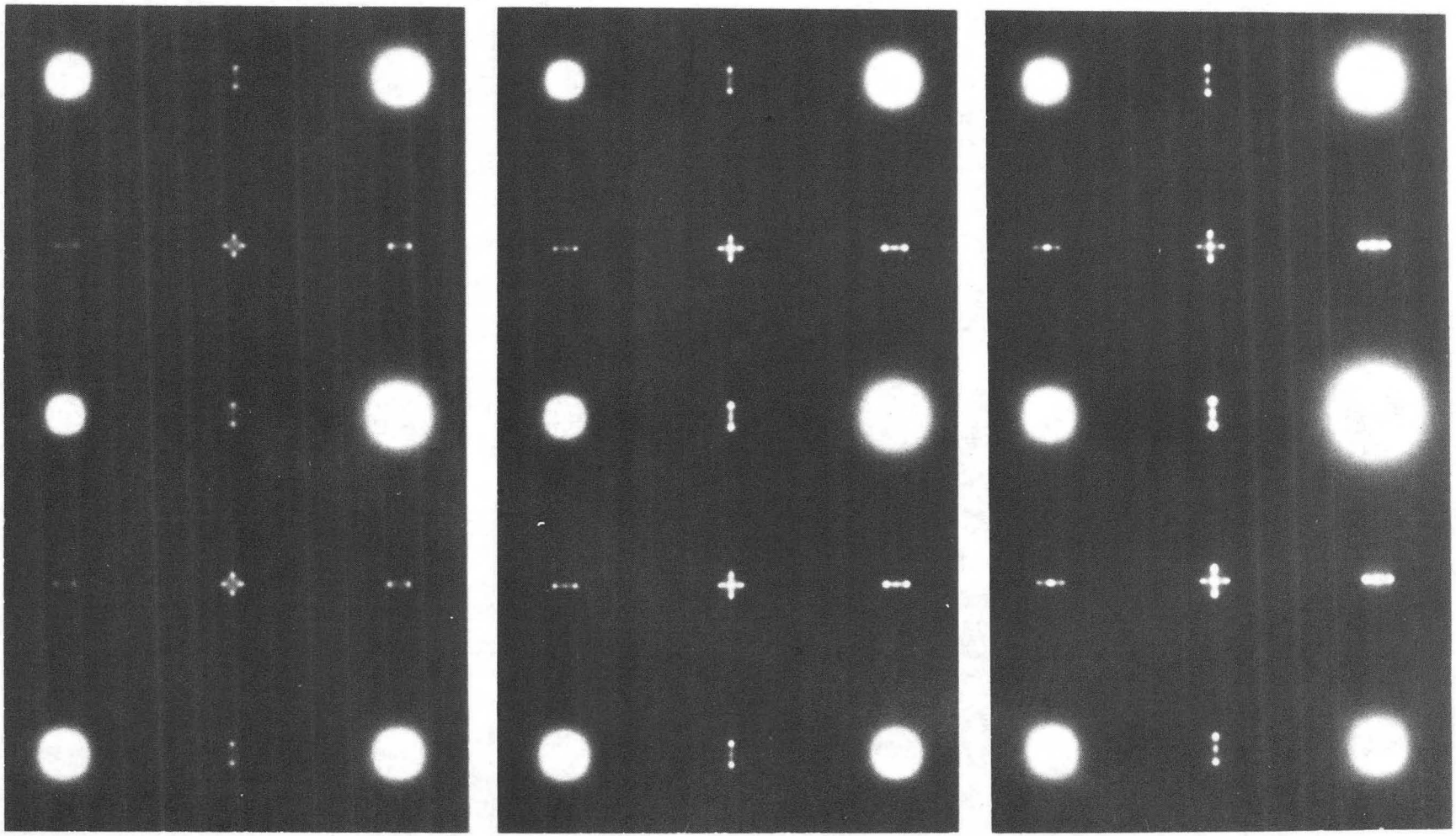

XBB 855-4051

Fig. 7

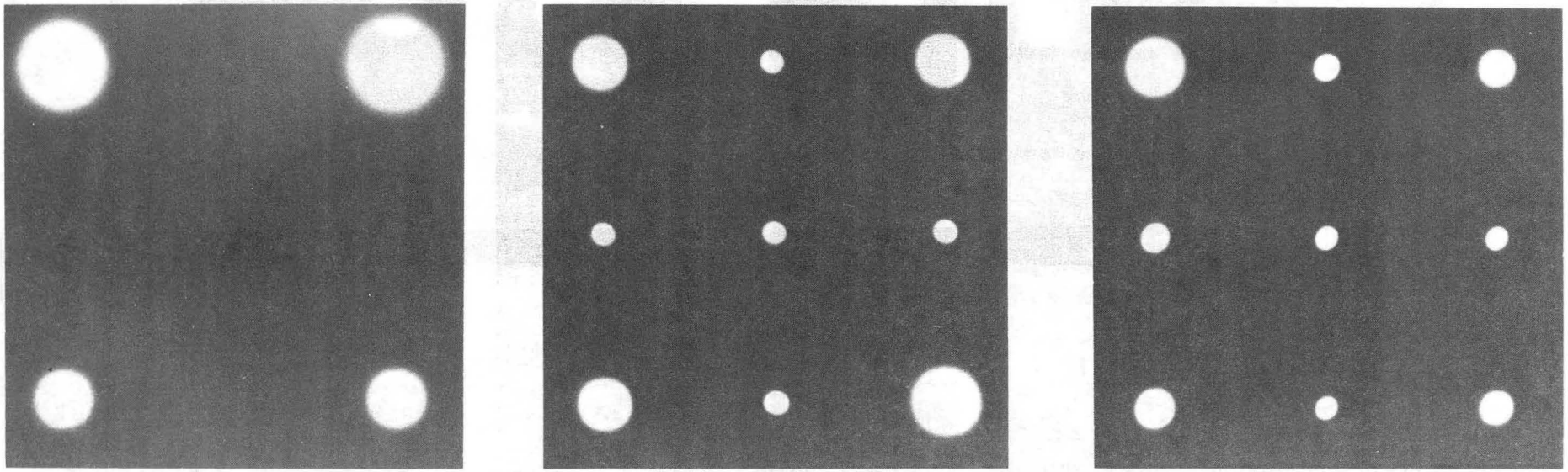

20°C 250°C 400°C

XBB 850-8128A

Fig. 8

16%

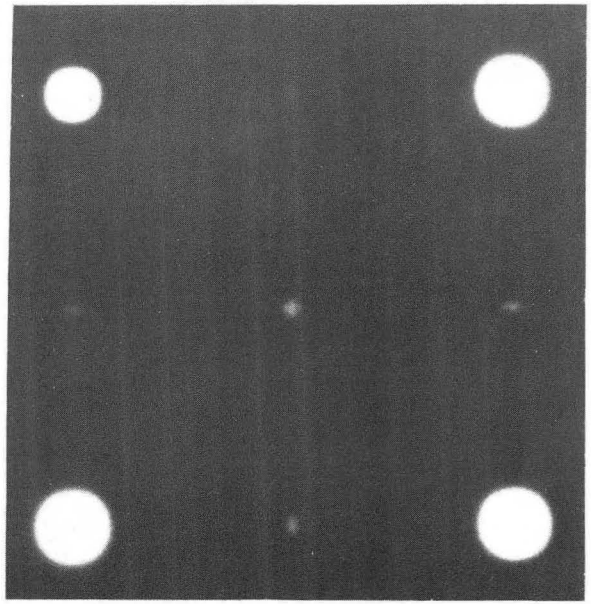

20°C

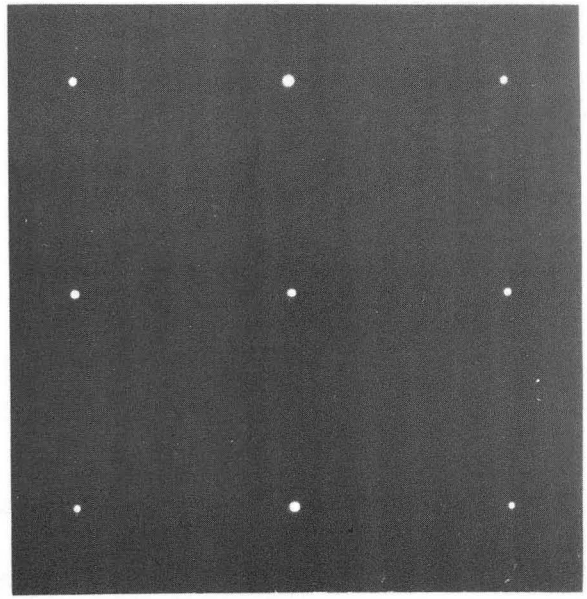

360°C

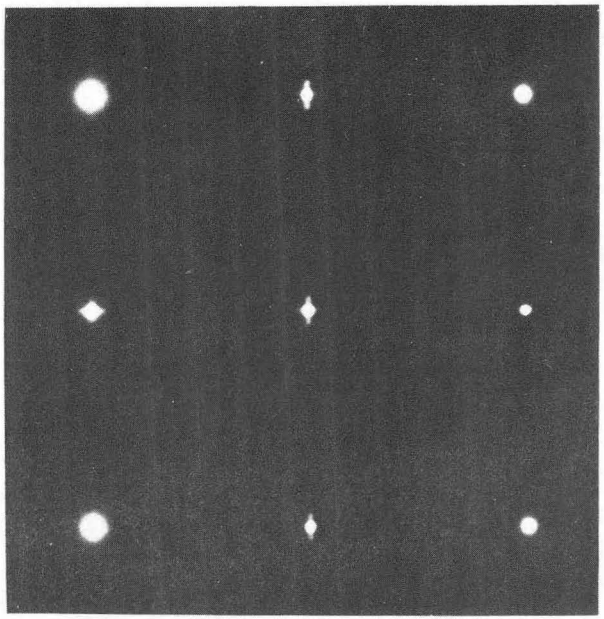

465°C

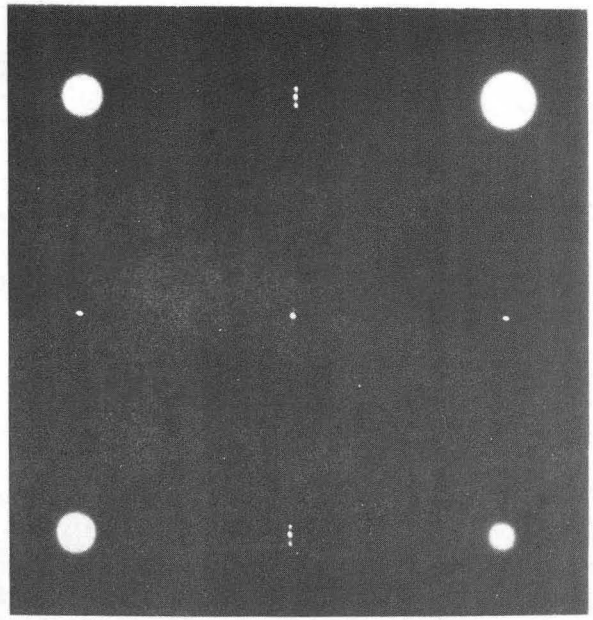

485°C

18%Pd

Fig. 9

XBB 850-8127

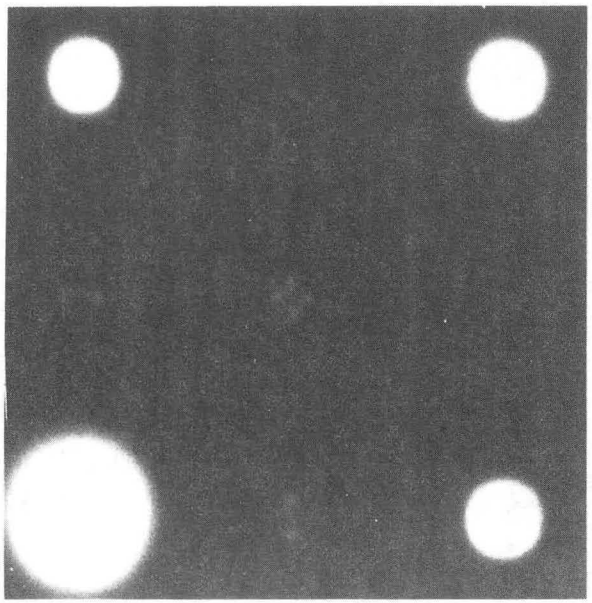

20°C

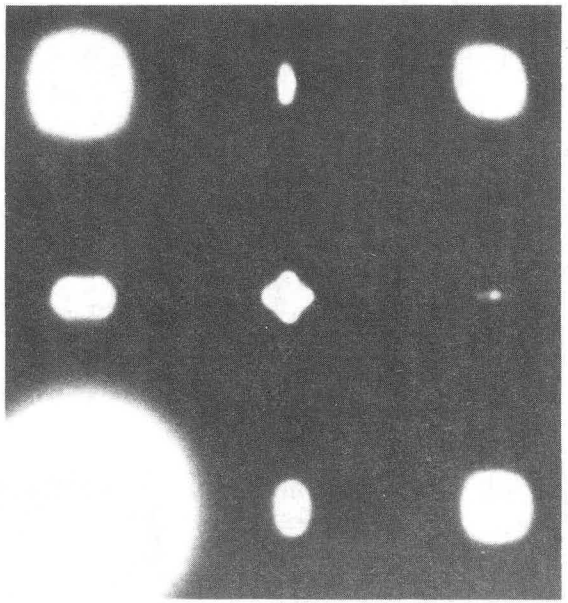

300°C

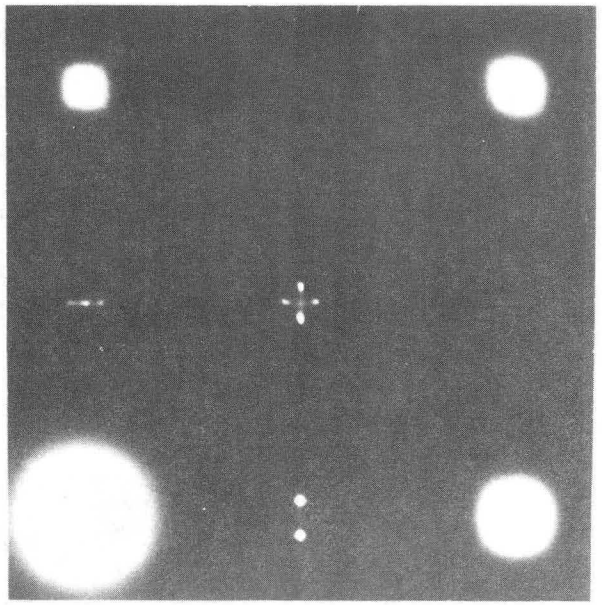

464°C

Fig. 10

XBB 850-8126A

22%Pd

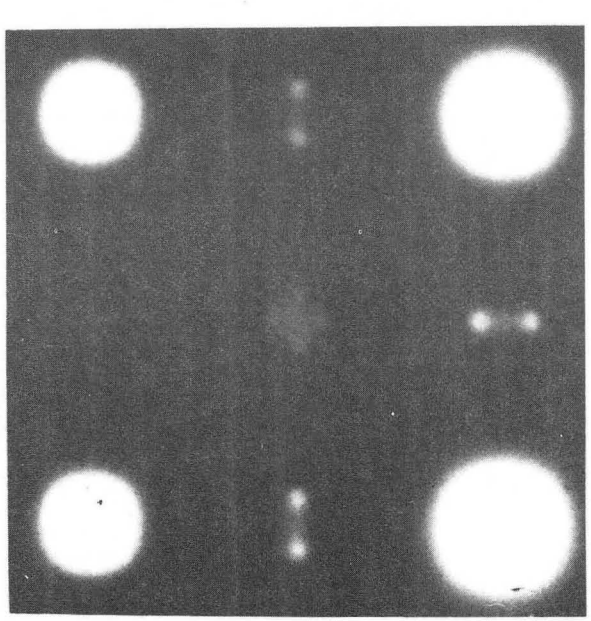

21°C

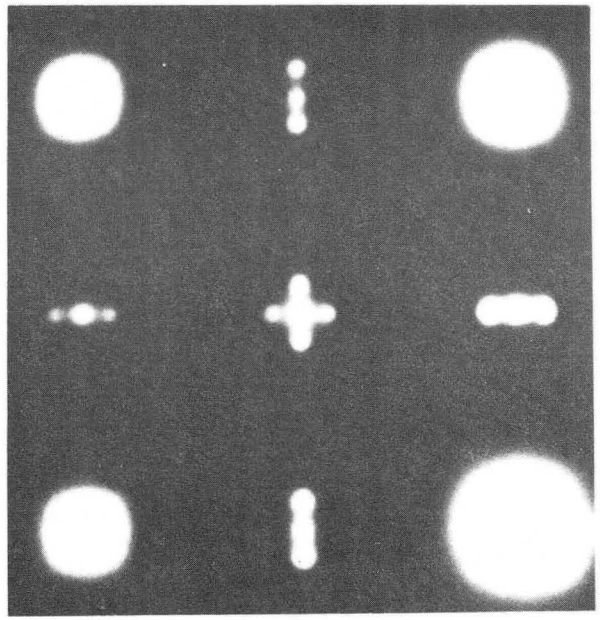

427°C

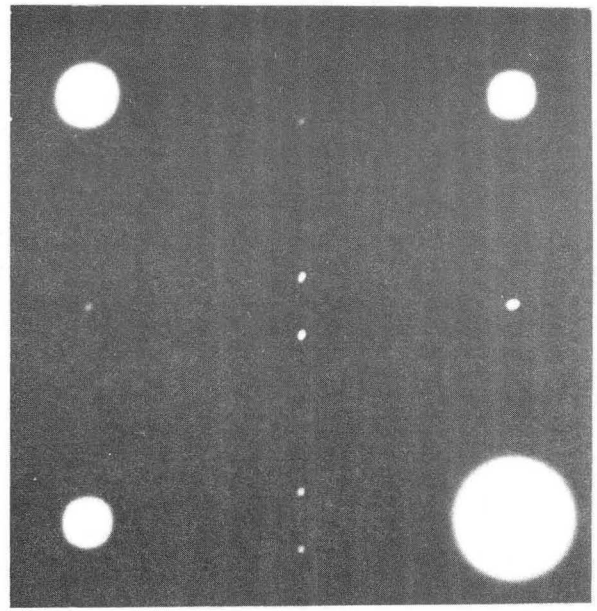

466°C

Fig. 11

XBB 867-5905

26%Pd

LAWRENCE BERKELEY LABORATORY
TECHNICAL INFORMATION DEPARTMENT
UNIVERSITY OF CALIFORNIA
BERKELEY, CALIFORNIA 94720